ELSEVIER

Journal of Nuclear Materials 306 (2002) 232–240

journal of nuclear materials

www.elsevier.com/locate/jnucmat

Plasma-driven superpermeation of hydrogen through Nb membranes: bulk effects

A.A. Skovoroda [a,*], V.S. Svishchov [a], A.V. Spitsyn [a], V.L. Stolyarov [a], Yu.M. Pustovoit [a], V.D. Borman [b], V.S. Kulikauskas [c], A.M. Shipilin [d]

[a] *Russian Research Centre, Kurchatov Institute, 123182 Moscow, Russia*
[b] *Moscow Engineering Physics Institute, Technical University, 115409 Moscow, Russia*
[c] *Skobeltsyn Institute of Nuclear Physics, Moscow State University, 119899 Moscow, Russia*
[d] *Yaroslavl State Technical University, Yaroslavl 150000, Russia*

Received 19 September 2001; accepted 10 October 2002

Abstract

A non-monotonic temperature dependence of the steady-state plasma-driven superpermeation of hydrogen through an Nb membrane is observed for the first time. Such a permeation behavior is related not only to the surface properties of the membrane, but also to its bulk properties and defects.
© 2002 Elsevier Science B.V. All rights reserved.

PACS: 52.40.Hf; 66.30.−h; 68.45.Da; 68.35.Rh

1. Introduction

As is known [1,2], the permeation efficiency of equilibrium molecular hydrogen through vanadium-group (V, Nb, and Ta) metallic membranes is extremely low in comparison with that of the non-equilibrium hydrogen. Under steady irradiation of the inlet side of the membrane by a flow of hydrogen atoms or ions (with flux densities j_a or j_i, respectively) that are produced by the dissociation (ionization) of equilibrium molecular hydrogen, a flow of equilibrium molecular hydrogen with the flux density $j_{H_2} = 0.5\eta j_{a,i}$ (where η is the permeation efficiency) is observed on the outlet side. The value of the permeation efficiency can be close to unity. The physical reason of such a phenomenon, which is called 'superpermeation', consists in the combination of the large absorption and small desorption probabilities under conditions, such that the membrane bulk operates as a trap for gas particles. Great interest in this phenomenon is motivated by its possible unique technological applications, especially, in fusion research [3–6]. However, till now, the effect of superpermeation through metal membranes have not yet been widely employed.

The complexity of the practical application of superpermeation can partially be explained in terms of the existing classical theory, which is based on surface physics. It is well known (see, e.g. [1,2]) that the formation of a surface barrier (SB), whose energy depends on the surface cleanness, affects strongly the processes of hydrogen input in (output from) the Nb membrane. If the energy of a non-equilibrium particle is above the SB energy, then hydrogen easily dissolves in the bulk of the Nb membrane. Sivert's law, $j_{H_2} = KC^2$, describes the release of hydrogen from the membrane volume. Here and below, we use the notation of [7]: C is the concentration of the dissolved hydrogen atoms close to the membrane surface (C_0 at the inlet surface, irradiated by the flow of non-equilibrium particles, and C_L at the outlet surface) and K is the recombination coefficient (K_0 on the inlet side and K_L on the outlet side). The recombination coefficient K depends strongly on the

* Corresponding author. Fax: +7-95 943 00 73.
E-mail address: skovorod@nfi.kiae.ru (A.A. Skovoroda).

0022-3115/02/$ - see front matter © 2002 Elsevier Science B.V. All rights reserved.
PII: S0022-3115(02)01324-7

surface cleanness and cannot be controlled with a high accuracy, especially for Nb membranes [8]. By solving the steady-state one-dimensional diffusion problem [7], it is easy to obtain an expression for the permeation efficiency in the case of a thin membrane and low flux densities ($C_0 - C_N \ll C_0$, $\beta = D/L\sqrt{Jk_0} \gg 1$, where D is the coefficient of hydrogen diffusion, L is the membrane thickness, and J is the flux density of non-equilibrium particles). By introducing the dimensionless parameter $\gamma = K_L/K_0$, the efficiency η can be written as [1,2,7]:

$$\eta = \frac{\gamma}{\gamma + 1}. \tag{1}$$

For an Nb membrane with a thickness of 0.1 mm and at a hydrogen flux density of 100 A m^{-2}, expression (1) is valid at room temperature. In these estimates, the following approximations for D and K were used [8–10]:

$$D\ [\mathrm{m^2\,s^{-1}}] = 5.9 \times 10^{-8} \exp(-1300T^{-1}\ [\mathrm{K}]),$$
$$K\ [\mathrm{m^4\,s^{-1}}] = 4 \times 10^{-25} \exp(-13\,000T^{-1}\ [\mathrm{K}])$$

which are valid in the temperature ranges $T = 180$–850 and 500–1000 K, respectively.

Classical relation (1) shows that the permeation through a thin Nb membrane should possess the following features: (i) superpermeation occurs for $\gamma \sim 1$ or higher, i.e., when the SB energy on the inlet side is close to or higher than that on the outlet side; (ii) the superpermeation efficiency η does not depend on the membrane thickness, temperature, particle flux density, and diffusion coefficient; and (iii) the volumetric membrane properties do not directly affect the superpermeation efficiency.

The above features of superpermeation were observed in experiments with Nb membranes [1–6] under certain conditions, such as thorough sample cleaning by long annealing at a temperature of 2000 K under ultrahigh vacuum and the use of atomic (rather than ionic) hydrogen at fairly high membrane temperatures of $T \sim 1000$ K. The physical reasons for these conditions are clear. The first condition stems from the necessity of removing impurities from the Nb surface. The cleaning of the membrane and the reduction of oxides and other compounds is obligatory. The necessary degree of cleaning is discussed below. Note that the theory [1,2] predicts the disappearance of superpermeation not only for thick impurity layers, but also for an ideally cleaned inlet surface (see (1)). The second condition is related to the preservation of a thin impurity layer on the inlet surface from irradiation. The hydrogen atoms have small, but sufficient energies to overcome the SB without destroying it, whereas the plasma ions, which have higher energies, can destroy the SB. The high temperature is necessary to eliminate the bulk effects.

This work is aimed at studying plasma-driven superpermeation at relatively low (lower than 1000 K) temperatures, when the bulk properties of the membrane material play a significant role. Such an investigation is of interest because the plasma-driven production of intense non-equilibrium hydrogen flows has the highest efficiency. The intense plasma flow destroys the SB on the inlet side; hence, according to the classical theory, superpermeation should disappear. However, this prediction contradicts to experiments [11,12]. To explain the experimental observations in terms of the classical theory, the authors of [12] put forward the hypothesis that the SB on the inlet side is preserved due to either impurity segregation from the membrane volume or an impurity flow from an insufficiently pure plasma. However, the existence of such an SB is possible only at low densities of the plasma flow. In this work, it is shown that the steady-state plasma-driven superpermeation is also observed at fairly high densities of a pure plasma flow. Under these conditions, the cleaning rate exceeds the impurity segregation rate.

2. Experimental facilities

Two experimental installations were used in experiments with Nb membranes. The first installation (In1) was applied to study the temperature dependence of hydrogen permeation at intensive plasma irradiation. The second installation (In2) was used to measure the sorption and desorption of equilibrium hydrogen.

2.1. In1 installation

The device was to obtain a steady-state pure hydrogen plasma flow with a large diameter and a high flux density exceeding the atomic flux density. For this purpose, a microwave distributed electron-cyclotron-resonance (DECR) plasma source is used. Such a source has many applications in microelectronics [13]. The parameters of our DECR source are given in Table 1.

In the experiments described, the ability of the DECR source to provide an intense flux of pure plasma at a low gas pressure of 0.01 Pa was employed. Under these conditions, the atomic flux is lower than the ionic flux. Previous experimental investigations of the plasma parameters in the DECR source allowed us to develop the code OGRAS for calculating H^0, H^+, H_2^+ and H_3^+ fluxes. The code uses the measured parameters, such as the gas pressure P, the electron temperature T_e, and the ion current density j_{ion} onto a floating Langmuir probe. A representative example of calculations is given in Table 2. When calculating the ion flux, we took into account the number of nuclei in a molecular ion. In experiment, it was possible to vary the membrane potential (within $\pm$400 V) and, hence, the energy and type of the particles (ions or electrons) bombarding the membrane.

Table 1
DECR plasma source parameters

Parameter	Value
Maximum ion current density (A/m^2)	100
Ion energy (eV)	>10
Flow diameter (m)	0.15
Flow inhomogeneity (%)	2
Flow time stability (% per hour)	5
Flow fluctuations (%)	5
Magnetron frequency (GHz)	2.45
Magnetron power (kW)	1
Number of waveguide electrodes	8
Type of permanent magnets	NdFeB
Gas pressure (Pa)	10^{-3}–10^{-1}
Ultimate vacuum (Pa)	10^{-5}
Vacuum chamber	Without warming

Table 2
Fluxes in a discharge with parameters $P = 0.07$ Pa, $T_e = 4.1$ eV, and $j_{ion} = 17$ A/m^2

Parameter	Value
H^0 density, 10^{16} m^{-3}	6
H^+ density, 10^{16} m^{-3}	0.1
H_2^+ density, 10^{16} m^{-3}	0.2
H_3^+ density, 10^{16} m^{-3}	1
H^0 flux, 10^{20} atom/m^2 s	0.8
Ion flux, 10^{20} atom/m^2 s	2.5
Maximum permeation flux, 10^{20} atom/m^2 s	0.8
H_2 sorption rate, 10^{20} atom/m^2 s	0.05

The flux of molecular hydrogen leaving the membrane from the outlet side was measured by means of a diaphragm with a gas conductivity of 3 s^{-1}. Two gauges measured the pressure difference at the opposite sides of the diaphragm. The gas composition was monitored by a quadrupole mass-analyzer. Fig. 1 shows a schematic of the In1 vacuum system.

A 50-mm-diameter membrane for permeation experiments was fabricated by pressing an Nb foil between two flanges. To isolate the foil from the metal flange, MgO paste was used. The membrane was heated by using a dc power supply. The temperature was measured by five thermocouples welded at the center and at the edge of the membrane and at the middle of the membrane radius. The radial variations in the membrane temperature did not exceed 50 K at dc heating up to 1000 K.

The mechanical properties of the Nb foil were investigated by using acoustic measurements. For this purpose, the membrane block schematically shown in Fig. 1 was replaced with a special acoustic block described in [6,14].

2.2. In2 installation

The In2 ultrahigh-vacuum installation was used to study the equilibrium-hydrogen sorption by (desorption from) Nb membranes. Samples made from an Nb foil of size 160×15 mm^2 were placed in a 75-l warmed-up volume with a background gassing of 10^{-6} 1Pa/s. The samples were heated up to a temperature of 1300 K. A schematic of the In2 vacuum system is shown in Fig. 2.

Two types of dynamic measurements of the sorption and desorption processes in Nb membranes at low gas pressures were performed. The dependence of the hydrogen pressure on the membrane temperature was measured with and without pumping.

Hydrogen sorption by (desorption from) Nb has been investigated by many authors (see, e.g. [8,15]). All the authors paid special attention to cleaning the sample surface. In our experiment, we both cleaned the sample surface by ion sputtering and contaminated it by oxidation. The membrane biasing in an argon discharge leads to sputtering, whereas the heating in oxygen leads to surface oxidation.

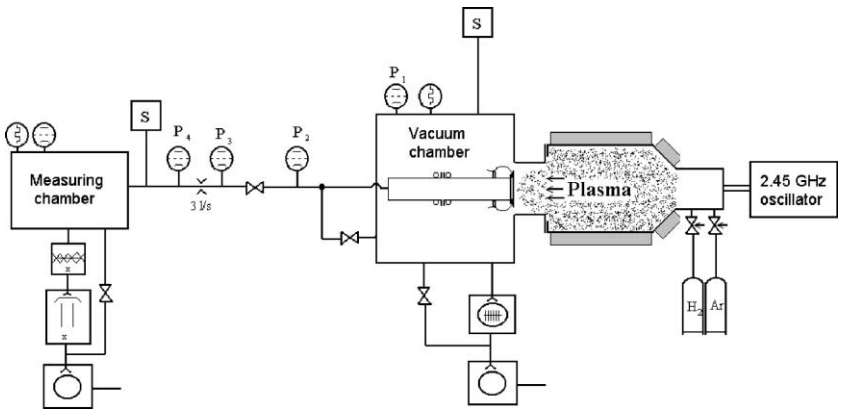

Fig. 1. Schematic of the In1 vacuum system: (*P*) vacuum gauge and (*S*) mass-analyzer.

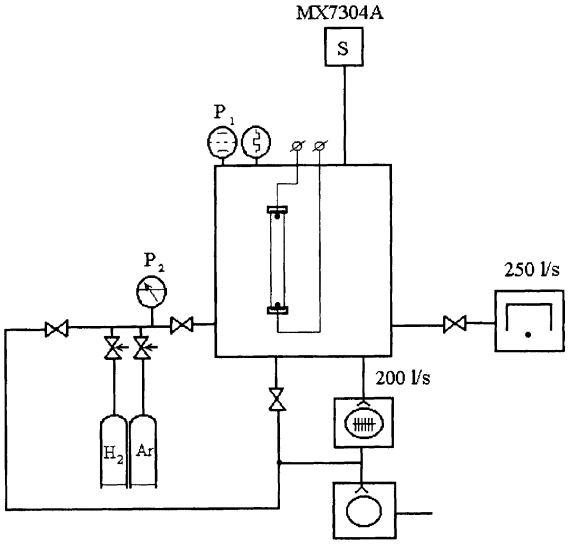

Fig. 2. Schematic of the In2 vacuum system.

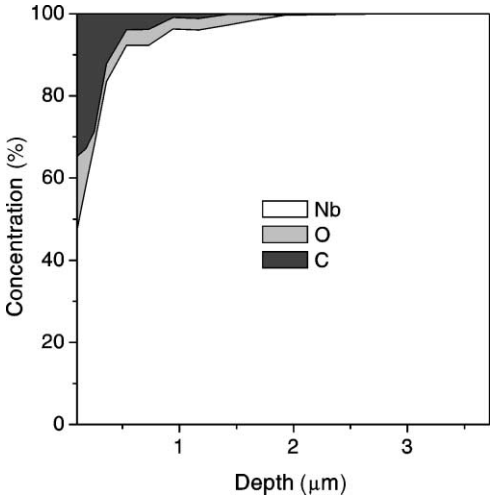

Fig. 3. Profiles of the Nb, O, and C concentrations near the surface of a 0.025-mm foil BDC.

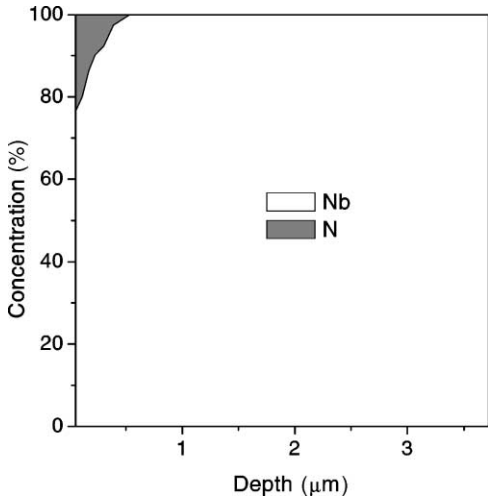

Fig. 4. Profiles of the Nb and N concentrations near the membrane surface after permeation experiments.

3. Nb membrane properties

We studied the properties of Nb membranes with thicknesses of 0.025 and 0.1 mm. The inductively coupled plasma (ICP) analysis showed the existence of 0.15% Ta in both membranes.

Membranes made from an Nb foil after its deep cleaning were only used. The procedure of cleaning consists of three steps: (i) the foil is cleaned in acetone, (ii) the foil is annealed in a vacuum at a temperature of 1300 K, and (iii) both sides of the foil are sputtered by an intense (30 A/m^2) flow of argon ions with energies of 800 eV. The duration of argon cleaning was chosen such as to ensure the sputtering of 2 μm of the foil. The profiles of the niobium, oxygen, and carbon concentrations in the original and cleaned foils are shown in Figs. 3 and 4. The profiles were measured by Rutherford backscattering (RBS) of a 7-MeV proton beam. Before RBS measurements, the samples were exposed to air. This exposure explains the appearance of a thin nitrogen surface layer in Fig. 4.

The quality of the surface was checked by the reproducibility of the measurements. Good reproducibility of experimental data was achieved only after the deep cleaning of the inlet and outlet surfaces and the periodical short argon cleaning of the inlet surface. We also used the sorption of oxygen at a pressure of 10^{-4} Pa to modify the surface. The influence of oxides on the sorption activity of metals is well known and is described in detail, e.g., in [16]. After oxidation, the vacuum characteristics of an Nb membrane changed substantially; however, short argon cleaning restored the previous membrane properties.

The outlet surface was cleaned only once. The gas pressure on the outlet side of the membrane never exceeded 100 Pa. To estimate how the quality of the outlet surface affected the phenomenon under study, a combined Nb/Pd membrane was fabricated whose outlet surface was covered with a 1-μm Pd film.

3.1. Distribution of hydrogen in a membrane

The hydrogen distribution in the original foil before deep cleaning (BDC) and in the membrane after permeation experiments was measured by using elastic recoil analysis (ERA). A helium beam with an energy of

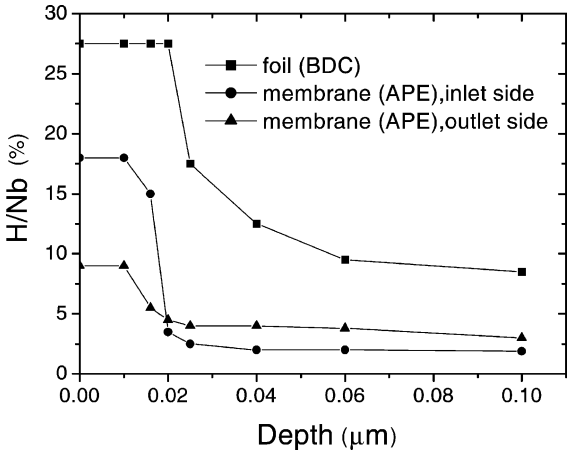

Fig. 5. Profiles of the hydrogen concentration near the surface of a 0.025-mm foil BDC and the membrane surface after permeation experiments (APE).

1.7 MeV was used for ERA. The detectable level of hydrogen was 1%. The results of these measurements are presented in Fig. 5.

We were interested in the distribution of hydrogen in the membrane body. Therefore, it was unnecessary to pay attention to the surface hydrogen that appeared due to the exposure of the membrane in air. The original foil contained a lot of hydrogen (~9%) in its volume. After the deep cleaning and permeation experiments, the density of hydrogen atoms in the membrane decreased. Note that the hydrogen density in the membrane near its outlet surface was appreciably higher than near the inlet surface, exposed by plasma. This paradoxical result has a simple explanation. The membrane was kept for 5–10 min at a rather high temperature in a good vacuum after plasma irradiation was terminated. Since the inlet surface was well cleaned by plasma, hydrogen could easily leave the membrane through this surface.

3.2. Crystal structure and phase transformations in the membrane

X-ray investigations of the original foil BDC and the membrane after permeation experiments allow us to draw the following conclusions. The original foil and the membrane are *textured*. In the original foil, the characteristic value of mechanical stress determined from the diffraction line width is $\delta a/a = 0.01$ (where a is the parameter of Nb crystal cell), which is ten times stronger than in the membrane.

It is known [17] that phase transformations in Nb affect strongly the attenuation of longitudinal acoustic waves. We investigated the $\beta \rightarrow \alpha$ phase transformation in the Nb–H system by using the longitudinal acoustic resonance at the frequency $f \sim 20$ kHz in a 9×80-mm^2 membrane. The dependence of the resonant line width Δf on the membrane temperature was measured. The membrane with piezoelectric gauges was located in the vacuum chamber of the In1 installation and was exposed to gas and plasma under various conditions (see [6,14] for details). A typical temperature dependence of $\Delta f/f$ for a 0.025-mm membrane is shown in Fig. 6.

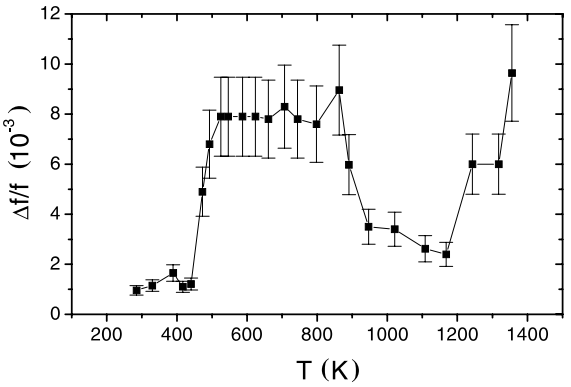

Fig. 6. Temperature dependence of the acoustic resonant line width $\Delta f/f$ for a 0.025-mm membrane.

Based on acoustic investigations, we can draw the following conclusions. A sharp increase in the resonant line width is observed at the critical temperature $T_c = 470 \pm 20$ K, which coincides with the temperature of the phase transformation of coupled hydrogen (β-phase) into mobile hydrogen (α-phase) [18]. Under our experimental conditions, the critical temperature did not depend on the membrane thickness and plasma exposure.

4. Experimental results

To investigate how the bulk properties affect superpermeation, Nb membranes of two thicknesses were used. The difference in the results obtained under the same experimental conditions demonstrates the bulk effects.

4.1. Plasma-driven superpermeation through Nb membranes

Hydrogen superpermeation through membranes with thicknesses of 0.025 and 0.1 mm was investigated in the In1 installation. The permeation efficiency at a fixed temperature was measured for several hours after switching-on the gas discharge. After the discharge was switched off, permeation rapidly disappeared.

Figs. 7 and 8 demonstrate the dependences of the steady-state permeation efficiency on the membrane temperature for 0.025- and 0.1-mm membranes, respectively. It can be seen that the permeation efficiency

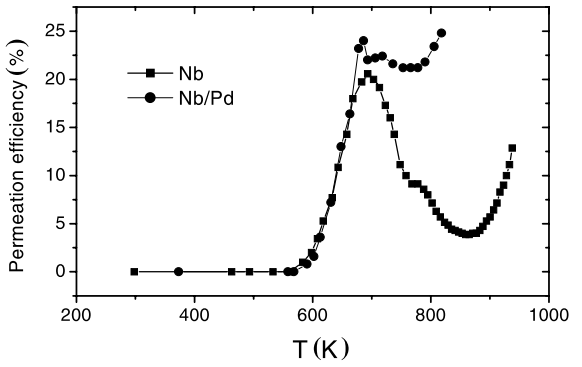

Fig. 7. Plasma-driven permeation efficiency η vs. temperature for 0.025-mm Nb and Nb/Pd (Nb covered with a 0.001-mm Pd layer on outlet side) membranes at the floating potential, an ion current density of 15 A/m^2, and a hydrogen gas pressure of 0.04 Pa.

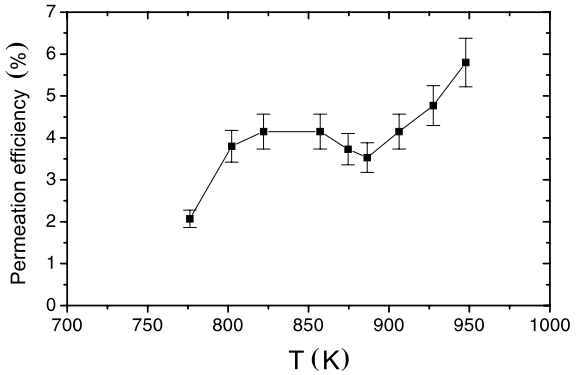

Fig. 8. Plasma-driven permeation efficiency vs. temperature for a 0.1-mm Nb membrane at a potential of −100 V, an ion current density of 17 A/m^2, and a hydrogen gas pressure of 0.04 Pa.

decreases in nearly inverse proportion to the membrane thickness. For the 0.025-mm membrane, superpermeation appears at a critical temperature of about 570 K. It is interesting that the temperature dependence is nonmonotonic. The efficiency increases with increasing temperature and reaches a local maximum, after which it somewhat decreases and, then, begins to grow again. The permeation efficiency depends slightly on the ion flux (in the range 1–30 A/m^2), the gas pressure in the outlet volume (in the range 0.001–0.1 Pa), and the membrane potential (in the range 0–100 V).

As the membrane temperature increases and then decreases, a hysteresis effect is observed. The temperature dependence of the permeation efficiency for three cycles of heating is shown in Fig. 9. The time during which steady-state permeation is reached is a few minutes for the 0.025-mm membrane at a temperature of 670 K. For the 0.1-mm membrane, this time is a few tens of minutes at a temperature of 770 K. Therefore, it is

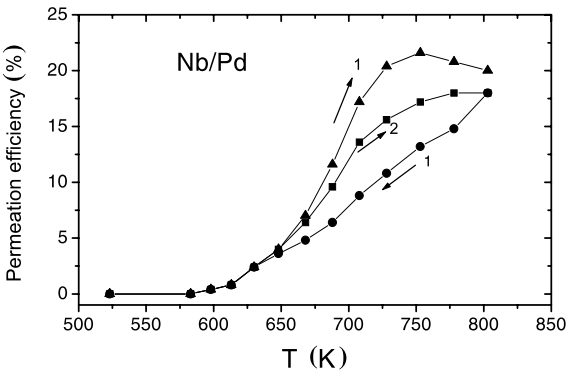

Fig. 9. Dynamics of the plasma-driven permeation efficiency for an Nb/Pd membrane: (1) the first cycle of heating and cooling and (2) the second cycle of heating; the heating rate is about 15 K/min, the ion current density is 13 A/m^2, the membrane potential is −10 V, and the hydrogen pressure is 0.06 Pa.

only worth to carry out dynamic experiments with thin membranes.

The measurements of steady-state permeation show a small degradation of the efficiency (about 1% per hour). After 1-min argon cleaning, the permeation efficiency restores. Both the permeation efficiency and the degradation rate increase slightly with increasing negative membrane potential.

4.2. Molecular-hydrogen sorption by (desorption from) Nb membranes

The time dependences of the hydrogen pressure and the membrane temperature are shown in Fig. 10 for (a) high (without pumping) and (b) low (with pumping) pressure. One can see an identical behavior in low-temperature (400–800 K) and high-temperature (>1000 K) ranges. In these ranges, sorption at high pressure and desorption at low pressure are observed. In the intermediate temperature range, both sorption and desorption are significantly reduced. The conventional boundary between the low- and high-pressure ranges is about 3×10^{-4} Pa.

The following effects can be observed in low-temperature dynamic experiments. The reversibility of sorption and desorption processes is observed in experiments with a preliminary outgassed membrane. The amount of the absorbed gas increases as $\sqrt{P}$ at high pressures. The temperature corresponding to the most intense sorption at high pressures coincides with the temperature corresponding to the most intense desorption at low pressures. The temperature at which sorption (desorption) is the most intense depends on the heating rate. The higher the heating rate, the greater the temperature corresponding to the most intense sorption (desorption). At a constant pressure, the total amount of

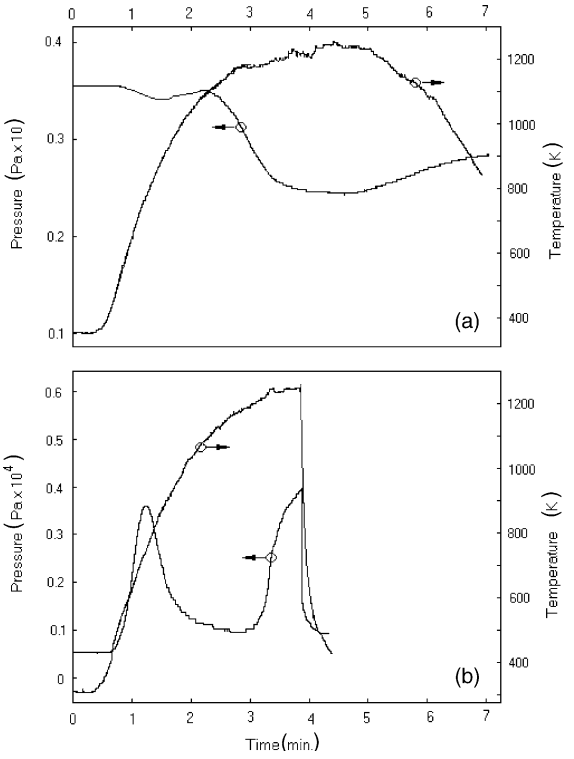

Fig. 10. Time behavior of the hydrogen pressure and the membrane temperature in the In2 installation (for a 0.025-mm Nb membrane after intensive argon cleaning): (a) high pressure (without pumping) and (b) low pressure (with pumping).

the absorbed gas is proportional to the membrane thickness (in the 0.1-mm membrane, the amount of the absorbed gas is by a factor of 4 higher than that in the 0.025-mm membrane).

The following effects can be observed in high-temperature dynamic experiments. At a temperature of 1000 K, intense desorption begins at low pressures (or sorption at high pressures). There is no reversibility of the sorption and desorption processes in this case. Only one-half of the previously absorbed hydrogen is desorbed at cooling.

Note that the measured sorption rate of molecular hydrogen is much lower than the fluxes of atoms and ions in plasma-driven permeation experiments (see Table 2).

5. Discussion

The main results of our measurements can be summarized as follows:

1. The permeation efficiency of equilibrium hydrogen through thin Nb membranes is very low in comparison with the efficiency of plasma driven permeation.
2. For Nb membranes, superpermeation in the low-temperature range is observed. It is characterized by the following properties: (i) the threshold temperature for the appearance of plasma-driven superpermeation is about 570 K (see Fig. 7), (ii) the threshold temperature for the appearance of a sharp peak of acoustic wave damping is about 470 K (see Fig. 6), (iii) the temperature dependence of the permeation efficiency is non-monotonic (see Figs. 7 and 8), and (iv) the temperature dependences of the gas sorption and desorption rates are non-monotonic (see Fig. 10).
3. The efficiency of plasma-driven permeation in the low-temperature range is inversely proportional to the membrane thickness.

The threshold temperatures appear to be close to the known temperature of the phase transformation in an H–Nb system, when the coupled hydrogen (β-phase) transforms into the mobile hydrogen (α-phase) [18]. Phase transformations were detected independently by acoustic and desorption measurements. The hysteresis effect observed in the permeation experiments also provides evidence in support of such transformations.

As was pointed out in [18], the $\beta \rightarrow \alpha$ phase transformation in a polycrystalline material is related to the behavior of hydrogen on the grain boundaries. At a threshold temperature of about 440 K (the phase transformation temperature depends on the amount of dissolved hydrogen and the surface cleanness), hydrogen atoms begin to diffuse along the grain boundaries faster than inside the crystallites. At lower temperatures, hydrogen atoms are captured at the grain boundaries (β-phase) and their diffusion rate becomes lower than inside the crystallites. Hence, permeation through polycrystalline membranes at low temperatures is strongly affected by the bulk defects. At high temperatures, the diffusion rate of hydrogen atoms along the grain boundaries and that inside the crystallites both increase; hence, in this case, the regime of classical superpermeation can be realized.

5.1. Non-monotonic temperature dependence of permeation

The most typical experimental result is the non-monotonic temperature dependences of the permeation efficiency and the sorption (desorption) rate of hydrogen in thin Nb membranes in the low-temperature range. The following hypotheses can be proposed to explain this phenomenon.

The first hypothesis. Remaining within the classical permeation theory [1,2,7], we should redefine the diffusion and recombination coefficients in order to take into account the processes on the grain boundaries. The experimentally measured decrease in the efficiency of plasma-driven permeation with increasing membrane

thickness allows us to conclude that diffusion limits the hydrogen permeation ($C_L \ll C_0$, $\beta \ll 1$) [7]. In this case, the permeation flux j can be estimated as $j = DC/L$. For example, using the value of the hydrogen solubility in Nb from [19] to determine the hydrogen atom density C and the diffusion coefficient D, specified in the introduction, we obtain $j \sim 10^{21}$ atom/m^2 s for a 0.02-mm membrane at a temperature of 570 K. The estimated permeation flux is larger than the measured maximum plasma-driven permeation flux (see Table 2).

The small β value can be achieved either by substantially reducing the diffusion coefficient D or by increasing the recombination coefficient K with respect to their values specified in the introduction. At temperatures below the threshold temperature, the diffusion coefficient of β-hydrogen is supposed to be very small and the parameter β is much less than unity. During the phase transformation, the diffusion coefficient for hydrogen atoms increases rapidly. As a result, the parameter β and the permeation efficiency also increase. A further increase in the temperature results in a decrease in the parameter β if the activation energy of recombination is greater than the double activation energy of diffusion (e.g., this is true for the values specified in Section 1). The decrease in β will result in the observed decrease in the permeation efficiency. The change of the activation energy of recombination can explain the absence of a substantial decrease in the permeation efficiency in the experiments with a combined Nb/Pd membrane (see Fig. 7).

The main drawback of this hypothesis is the assumption that, for plasma-driven experiments, the recombination coefficient on the outlet surface is much higher than that specified in Section 1. We remind that, in our case, the outlet surface was cleaned only once at the beginning of experiments.

The second hypothesis. We assume that the grain boundaries form a network of connected 'channels' (CCs) in the bulk of the membrane. The network can have 'open channels' (OCCs) on the surface.

Many phenomena observed in the low-temperature range can be qualitatively explained based on this assumption. Careful surface cleaning is necessary for the formation of open channels. If the network has OCCs, then the phase transformation in a CC should be accompanied by the desorption of hydrogen. In fact, we observed this effect, but only after intensive argon cleaning. The reversibility of the sorption and desorption processes is also related to the network. It can explain the observed increase in the sorption capacity with increasing membrane thickness. The CC-percolation phase transformation explains the threshold temperature for plasma-driven superpermeation. A textured thin membrane should facilitate percolation.

The theory of molecular gas diffusion in one-dimensional subnanometer channels [20] can be used to demonstrate the non-monotonic temperature dependence of the permeation efficiency. Note that, in our experiment, hydrogen atoms diffuse in CCs. This is confirmed by the observed square-root dependence of the sorption rate on the gas pressure. The CC transverse dimension is supposed to be so small that only one hydrogen atom can be placed within it. Thus, a chain of hydrogen atoms can be disposed along the channel. The displacement of one atom causes the displacement of all atoms in the dense chain.

In [20], an expression for the channel diffusion coefficient was derived. The authors designed the temperature function $\theta(T) = \sigma q/L$, which describes the degree of channel filling by particles. Here, σ is the atom diameter, L is the channel length, and q is the number of particles in the channel. The diffusion coefficient is

$$D(T) = D_0\left(1 + \frac{\theta^2}{(1-\theta)^2}\right), \tag{2}$$

where D_0 is the usual diffusion coefficient. One can see that the channel diffusion is faster than usual diffusion and its temperature dependence can be non-monotonic.

The above model is very simplified, because there are many other factors that are to be taken into account. The grain boundaries are the most obvious type of the bulk defects in polycrystalline metal membranes. The dislocation network can also be formed due to the intensive irradiation of a membrane during cleaning [21]. These dislocations tend to grow in the course of irradiation. The dislocation 'length' can be comparable with the membrane thickness. The diffusion along the dislocation is fast and can have a non-monotonic temperature dependence [22].

6. Conclusion

Our experiments with thin Nb membranes have shown that there are a lot of factors that govern plasma-driven superpermeation in the low-temperature range. Material defects and phase transformations determine the non-monotonic character of the temperature dependence of the permeation efficiency. The efficiency of steady-state plasma-driven permeation increases with decreasing the membrane thickness. A maximum efficiency of 25% has been obtained. Argon cleaning increases the efficiency of plasma-driven permeation in the low-temperature range.

Acknowledgement

We thank Professor A.A. Pisarev for fruitful discussions.

References

[1] A.I. Livshits, Zhurnal Tekhnicheskoi Fiziki 45 (1975) 1915 (Sov. J. Tech. Phys. 20 (1975) 1207).
[2] A.I. Livshits, M.E. Notkin, A.A. Samartsev, J. Nucl. Mater. 170 (1990) 74.
[3] A.I. Livshits, Vacuum 29 (1979) 103.
[4] A.I. Livshits, Yu.M. Pustovoit, V.S. Svishchov, Voprosy Atomnoi Nauki i Tekhniki, Ser.: Termoyad. Sintez (Topics in Atomic Science and Technology, Ser.: Thermonuclear Fusion, in Russian) 2 (8) (1981) 45.
[5] Proceedings of Japan-CIS Workshop on Interaction of Fuel Particles with Fusion Materials (IFPFM), every year since 1992.
[6] C.H. Wu (Ed.), Hydrogen Recycling at Plasma Facing Materials, 177, Kluwer Academic Publishers, Netherlands, 2000.
[7] A.A. Pisarev, V.M. Smirnov, Atomnay Energiya (Atomic Energy, in Russian) 61 (1986) 178.
[8] V. Bandourko, M. Yamawaki, K. Yamaguchi, et al., J. Nucl. Mater. 233–237 (1996) 1184.
[9] B.A. Kolachov, Yu.V. Levinskii, M. Metallurgiya, Konstanty zaimodeistviya metallov s gazami (Constants of gas metal interaction, in Russian), 1987.
[10] Y. Fukai, H. Sugimoto, Adv. Phys. 34 (1985) 263.
[11] Y. Fujii, H. Ishizuka, H. Nakano, et al., Proceedings of Japan-CIS Workshop on Interaction of Fuel Particles with Fusion Materials, Tokyo, 1992, p. 58.
[12] M. Bacal, A. Livshits, M. Notkin, et al., Proceedings of Japan-CIS Workshop on Interaction of Fuel Particles with Fusion Materials, Moscow, 1997, p. 24.
[13] J. Pelletier, in: O. Popov (Ed.), High Density Plasma Sources: Design, Physics and Performance, Noyes, Park Ridge, NJ, 1995, p. 380.
[14] A.A. Skovoroda, A.A. Spitsyn, Voprosy Atomnoi Nauki i Tekhniki, Ser.: Termoyad. Sintez (Topics in Atomic Science and Technology, Ser.: Thermonuclear Fusion, in Russian) 1 (2000) 84.
[15] S.M. Ko, L.D. Schmidt, Surf. Sci. 42 (1974) 508.
[16] V.D. Borman, S.V. Gubanov, Yu.Yu. Lebedinski, Yu.M. Pustovoit, et al., Proceedings of the 14th International Vacuum Congress, Birmingham, UK, 1998, p. 416.
[17] G.V. Zacharova, I.A. Popov, Niobiy i ego splavi (Niobium and its allows, in Russian), GNTIL chernoi i cvetnoi metallurgii, Moscow, 1961.
[18] V.A. Somenkov, S. Schilschtein, Hydrogen phase transformations in metals, Review IAE Kurchatov Institute, in Russian, Moscow, 1978, p. 1.
[19] S. Dushman, Scientific Foundations of Vacuum Technique, in: J.M. Lafferty, Wiley, New York, 1962.
[20] V.D. Borman, V.V. Tepluakov, et al., The molecular transport and sorption dynamic in subnanometer channels in ciolite membrane (in Russian), preprint MEPhI 001-2000, Moscow, 2000.
[21] Yu.V. Martynenko, P.G. Moskovkin, Radiat. Eff. Def. Solids 145 (1998) 39.
[22] Yu.V. Martynenko, P.G. Moskovkin, Proceedings of the 14th International Conference on Ion–Surface Interaction (ISI-14), Zvenigorod, Russia, vol. 2, 1999, p. 57.